

PAPER • OPEN ACCESS

Time-delay compensation and weighted feedforward control for reducing current harmonic of grid-connected inverter in weak power network

To cite this article: Haitao Gao *et al* 2020 *IOP Conf. Ser.: Earth Environ. Sci.* **526** 012123

View the [article online](#) for updates and enhancements.

You may also like

- [Impact of heavy ion irradiation on CMOS current mirrors based on SOI and bulk Si substrates: mismatch and output impedance](#)
Weikang Wu, Xia An, Fei Tan et al.
- [Periodical discharge regime transitions under long-term repetitive nanosecond pulses](#)
Zheng Zhao, Chenjie Li, Xinlei Zheng et al.
- [Wideband mirrored current source design based on differential difference amplifier for electrical bioimpedance spectroscopy](#)
Fu Zhang, Zhaosheng Teng, Haowen Zhong et al.

ECS
The
Electrochemical
Society
Advancing solid state &
electrochemical science & technology

DISCOVER
how sustainability
intersects with
electrochemistry & solid
state science research

Time-delay compensation and weighted feedforward control for reducing current harmonic of grid-connected inverter in weak power network

Gao Haitao^{1*}, Wan Huaqing¹, Cui Qiguan¹, Liu Yiwen¹

¹Wuhan Second Ship Design and Research Institute, Wuhan 430064, China

*Corresponding author's e-mail: gaohaitao55@163.com.

Abstract: In order to improve the quality of grid-connected current, the full feed forward control of grid voltage is often used to increase the output impedance of inverter. However, due to the influence of digital control delay, not only the harmonic suppression effect is weakened, but also the negative phase shift of the output impedance, which deteriorates the stability of the inverter in the weak network. In this paper, a time-delay compensation and weighted feedforward control strategy is proposed, in which a series of quasi-resonant items are added to the full feed forward circuit, and only the feedforward background harmonics appear at the frequency. By designing the quasi-resonant term, not only the phase delay introduced by the digital control can be compensated, but also the higher output impedance at the background harmonic frequency can be obtained, and the negative phase shift of output impedance can be reduced, and to improve the stability of the inverter in a weak power grid. Finally, a 6kw inverter prototype is built, and the validity and correctness of the proposed control strategy are verified by experiments.

1. Introduction

Being one of the predominant means to develop and utilize renewable energy resources like wind energy, solar energy and others, the distributed generation is favorable to resolve energy shortages and environmental pollution. Meanwhile, as an interface between the renewable generation unit and the power grid, the grid connected inverter plays an essential role^[1] in converting the DC power into high-quality AC power, then feeding it into the power grid. With an increasing penetration of renewable energy and enlarging distribution of access location, it has presented a prevailing trend for low power grid application. For grid connected inverters, the impedance in power grid is an indispensable factor which varies within a broad range, thus bringing about great challenges^[2] for their steady operation. Additionally, abundant background harmonics exist in the power grid voltage. It would lead to current distortion, consequently hindering the connected grid from access to network^[3].

The output impedance of grid connected inverter should be increased to suppress the influence of background harmonics in power grid voltage, as well as to improve the quality of grid-connected current. Commonly it has two solutions: for one thing, raise the systematic loop gain^[4-6] at the background harmonic frequency. For instance, regulate the impedance by using the multi-resonant (PR) controller^[4, 5], or the proportional integral (PI) controller on the basis of various frequencies under synchronous rotating coordinates; For another, by imposing the feedforward voltage on the grid, it simulated one parallel impedance, thus rebuilding the output impedance^[7-9] of grid connected inverter.



In the midst of circuit implementation, the full feedforward voltage control^[8] in power grid could simulate paralleling impedance. This simulated impedance possessed the same amplitude as the output impedance of grid-connected inverter but in reversed symbol. Consequently, the rebuilt output impedance value was infinite^[10]; Nevertheless, digital control resulted in 1.5 beats of control delay^[11] so the full feedforward function contained lead link which couldn't be implemented physically. Accordingly, after reconfiguration, the amplitude value of output impedance for grid connected inverter couldn't be infinite. This phenomenon impaired the inhibitory effect on grid-connected current harmonics. What was worse, the feedforward strategy would bring about serious sensitivity on the power grid impedance so the system was inclined to be unstable^[10].

To minimize the impact caused by digital control delay, the most straightforward solution is adding an advanced phase compensation unit^[12-15] in the feedforward function. Nevertheless, none of above-mentioned methods can perfectly achieve advanced unit. Despite that inhibitory effect on grid-connected current harmonics has been improved, the system is still likely to operate unsteadily under weak power grid.

Proposed in the reference^[16], by reducing the feedforward weight in power grid voltage, it avoided presenting negative resistance characteristics within the latent frequency intersection band between the output impedance of grid connected inverter and the impedance of power grid. By this means, it improved the stability of grid connected inverter under weak power grid. Nevertheless, it sacrificed the inhibitory effect on current harmonics.

Showing consideration for both the inhibitory capability of grid connected inverter towards the current harmonics and also the stability under weak power grid, this thesis proposed a Time-Delay Compensation and Weighted Feedforward strategy (TDCWF for short). Depending on the rules that in power grid voltage, the background harmonic only appeared at integral multiple^[17] of the fundamental wave frequency; therefore, it only needed to feedforward the voltage components at the frequencies of background current harmonics to the control loop, meanwhile to compensate the phase lag caused by digital control delay. By this means, it effectively ensured the inhibitory effect on grid-connected current harmonics. Additionally, within the latent frequency intersection band between the output impedance of grid connected inverter and the impedance of power grid, the feedforward weight in grid voltage was decreased to guarantee systematic stability under weak power grid.

2. Operating Principle of Time-Delay Compensation – Weighted Feedforward Control in Power-Grid Voltage

In the wake of references^[10] and^[16], it used the derived cancellation term expression $FC(s)$ which was introduced by full feedforward control in grid voltage. By comprehensive analysis, it obtained the feedforward cancellation term expression in power grid voltage as $FC''(s)$:

$$FC''(s) = \sum_k R_k(s) \cdot FC(s) \quad (1)$$

where $R_k(s)$ represented the quasi-resonant term which was added at the k-times frequency of current harmonics. It was expressed as:

$$R_k(s) = \frac{2K_{rk}\omega_{rk}s}{s^2 + 2\omega_{rk}s + (\omega_{rk})^2} \quad (2)$$

K_{rk} represented the coefficient of resonance term; ω_{rk} represented the bandwidth of resonance term, ω_{rk} represented the frequency of characteristic angle. It is necessary to point out that, here k could be selected as per actual grid-connected current harmonics to be inhibited. In case the bandwidth value of resonance term was relatively smaller, the gain value of $R_k(s)$ at both sides of characteristic frequency ω_{rk} spiraled down relatively faster. The gain value at other frequency of current harmonics was very small. Therefore, the intersection between quasi-resonant terms could be negligible. Near the k-times frequency of current harmonics, the cancellation vector could be set approximately as:

$$FC''(j\omega) = R_k(j\omega) \cdot FC(j\omega) \quad (3)$$

Here, the characteristic angle frequency of quasi-resonant term ω_{rk} was purposely set a bit higher than

k-times harmonic angular frequency ω_k . It aimed at using the positive phase ahead of its characteristic frequency to compensate the negative phase $\Delta\phi$ of $FC(j\omega_k)$. However, further observation on Figure 1 shown that, the phase value of $R_k(j\omega)$ decreased when the frequency is slightly higher than ω_k , and the gain value was still relatively larger. This meant in spite that the lagging phase of cancellation phasor $FC(j\omega_k)$ at ω_k frequency could be adequately compensated, it still had lagging phase at frequencies where were higher than ω_k . This brought about negative phase shift on output impedance $Z_{o_ff}(j\omega)$ of grid-connected inverter in correspondence with $Z_o(j\omega)$.

In case $\omega_k < 2\pi f_d$, though the negative phase shift occurred in the output impedance, however, the amplitude frequency curves of $Z_g(s)$ and $Z_{o_ff}(s)$ wouldn't intersect within this frequency band. Therefore, systematic stability would not be affected. Under such circumstances, the resonance coefficient K_{rk} was supposed to be tweaked as $|R_k(j\omega_k)| = K_{rk} = 1$ to guarantee its inhibitory effect on grid-connected current harmonics. Ideally, by using Time-Delay Compensation – Weighted Feedforward control strategy, the output impedance of grid connector inverter $Z_{o_tcwf}(j\omega_k)$ at k-times harmonic frequency was infinite. That was, the grid-connected current would not be affected by k-times harmonics in power grid voltage at all.

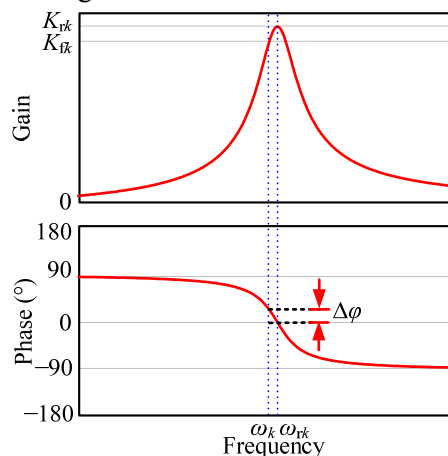


Figure 1 Frequency Characteristics Drawing of Quasi-Resonant Terms

In case $\omega_k \geq 2\pi f_d$, it may bring about interaction between the output impedance of grid connected inverter and the output impedance of power grid. To ensure the system to operate stably, it should select workable K_{rk} to minimize the negative phase shift of output impedance. The phasor diagram was drawn to illustrate the influence of voltage feedforward in power grid. It was shown in Figure 2. Based upon the sine theorem, it obtained:

$$\frac{1}{\sin \gamma} = \frac{|FC''(j\omega)|}{\sin \Delta\theta} = \frac{|R_k(j\omega)|}{\sin(\Delta\theta)} \tag{4}$$

In the expression, γ represented the included angle between $FC''(j\omega)$ and $1 - FC''(j\omega)$; $\Delta\theta$ represented the positive phase of $1 - FC''(j\omega)$, i.e. the negative phase shift of $Z_{o_tcwf}(j\omega)$ in correspondence with $Z_o(j\omega)$.

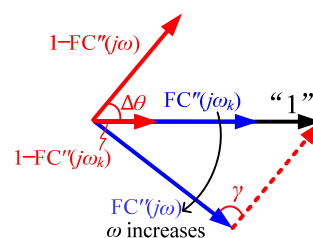


Figure 2 Phasor Diagram under the Influence of Time-Delay Compensation – Weighted Feedforward in Power Grid Voltage

According to expression (4), it could obtain:

$$\sin(\Delta\theta) = |R_k(j\omega)| \cdot \sin\gamma \quad (5)$$

As $|FC(j\omega)| < 1$ and $\Delta\theta$ was acute angle, so if $|R_k(j\omega)|$ equaled its maximum value K_{rk} (i.e. $\omega = \omega_{rk}$) as well as $\sin\gamma = 1$ ($\gamma = 90^\circ$), $\sin(\Delta\theta)$ possessed the maximum value, that was, $\Delta\theta$ was the largest. This would be the worst situation because $Z_{o_tcwf}(j\omega_{rk})$ possessed the maximum negative phase shift in correspondence with $Z_o(j\omega_{rk})$. In this case, the expression (5) could be revised as:

In consideration of ensuring system stabilization and certain phase margin PM, $Z_{o_tcwf}(j\omega_{rk})$ was supposed to meet:

$$\sin(\Delta\theta) = K_{rk} \quad (6)$$

where $\angle Z_o(j\omega_{rk})$ represented the phase of grid-connected inverter output impedance at ω_{rk} when feedforward control wasn't implemented in the connected grid.

$$\angle Z_{o_tcwf}(j\omega_{rk}) = \angle Z_o(j\omega_{rk}) - \Delta\theta \geq -90^\circ + \text{PM} \quad (7)$$

In the light of Equations (6) and (7), it obtained:

$$K_{rk} \leq \sin(\angle Z_o(j\omega_{rk}) + 90^\circ - \text{PM}) \quad (8)$$

To meet the requirements on stability, K_{rk} was supposed to take the maximum value to achieve the inhibitory effect on k-times current harmonics in connected grid.

In conclusion, by using Time-Delay Compensation – Weighted Feedforward Control Strategy in power grid voltage, it ensured the stability of grid connected inverter under weak power grid, and simultaneously enhanced the inhibitory effect on grid connected current harmonics as much as possible.

3. Parameter Design of the Time-Delay Compensation – Weighted Feedforward Control

3.1 Parameter Design on the Quasi-Resonant Terms

3.1.1 Design of Resonance Term Bandwidth ω_{ik}

In case the frequency of power grid fluctuated, the phase lag of $FC(j\omega)$ would not be precisely compensated. Accordingly, it weakened the inhibitory effect on grid-connected current harmonics. Suppose relatively larger bandwidth of resonance term was selected to improve the systematic adaptability on power grid frequency fluctuation, it may lead to serious coupling between the neighboring quasi-resonant terms. So, to design the characteristic angle frequency of $R_k(s)$ and its resonance term coefficient, it had to take the coupling impact from other resonance terms into account. This made the design process more complicated, even including repeated trial errors.

Therefore, this thesis presented the adaptively changeable quasi-resonant characteristic angle frequency ω_{rk} . It aimed at minimizing the value of ω_{rk} , consequently reducing the coupling between quasi-resonant terms. To compensate the phase, the characteristic angle frequency of quasi-resonant term at k-times current harmonics was set a bit higher than actual angular frequency at k-times current harmonics ω_k . The offset amount could be expressed as $\Delta\omega_k = \omega_{rk} - \omega_k$. Again, because $\omega_k = k\omega_o$, it could obtain ω_o in accordance with PLL, and adaptively set ω_{rk} as $k\omega_o + \Delta\omega_k$.

In real operation, error occurred in ω_o which was obtained from PLL, so the value of ω_{ik} couldn't be excessively small. Moreover, now that the error amount of ω_k was k times as that of ω_o , the ω_{ik} was supposed to be set as $k\omega_{io}$. Here, it might as well allow 1‰ error for ω_o that was obtained from PLL, and no more than 3° phase error for the quasi-resonant term, that was:

$$\begin{aligned} \angle R_1(j\omega_o \cdot (1 - 0.001)) &\leq 3^\circ \\ \angle R_1(j\omega_o \cdot (1 + 0.001)) &\geq -3^\circ \end{aligned} \quad (9)$$

Solve Equation (21) in accordance with Equation (15) to obtain $\omega_{io} \geq 1.91\pi$, here it took $\omega_{io} = 2\pi$, so $\omega_{ik} = 2k\pi$.

3.1.2 Design for the Characteristic Angle Frequency ω_{rk} and the Resonance Term Coefficient K_{rk}

ω_{rk} was adjusted to compensate the lagging phase of $FC(j\omega_k)$, and the K_{rk} was tweaked to introduce various weights at different current harmonic frequencies. Meanwhile, it took into account both the inhibitory effect on grid-connected current harmonics and also the system stability under weak power grid. Moreover, the design of $R_k(s)$ ought to consider the relationship of k -times current harmonics frequency and dividing frequency f_b . Under both circumstances, the design processes of ω_{rk} and K_{rk} in $R_k(s)$ were introduced as below.

1. k -times current harmonics frequency was lower than the dividing frequency,
In this case, $FC(j\omega_k)$ could be compensated by the unit vector "1", $R_k(s)$ was supposed to meet:

$$R_k(j\omega_k) \cdot FC(j\omega_k) = 1 \quad (10)$$

Solve the above equation to obtain the expected ω_{rk} and K_{rk} in design

2. k -times current harmonics frequency was higher than the dividing frequency

In this case, K_{rk} was determined in the wake of ω_{rk} . The purpose of design was compensating the lagging phase of $FC(j\omega_k)$. To realize that, $R_k(s)$ was supposed to meet:

$$\angle R_k(j\omega_k) = -\angle FC(j\omega_k) = 1.5\omega_k T_s \quad (11)$$

Solved above equation to obtain ω_{rk} ; then substituted ω_{rk} into equation (8) to get K_{rk}

3.2 Practical Case of Design

Followed by previously proposed design procedures, this chapter introduced a practical design case. Take the common frequencies in power grid voltage for instance, in specific; it selected the 3-times, 5-times and 7-times current harmonics within low frequency band, the 13-times and 21-times current harmonics within intermediate frequency band, as well as the 33-times current harmonics within high frequency band. Then quasi-resonant terms were added at these frequencies. Simultaneously, the quasi resonant term was also added at the fundamental frequency to reduce the grid-connected steady state error when the fundamental component in power grid voltage was introduced.

In the light of grid-connected inverter parameters shown in Table 2, it could solve to get $f_d \approx 486\text{Hz}$. This result represented the dividing frequency of latent intersection between the output impedance of grid connected inverter and the impedance of power grid. Here it proposed the design processes of $R_7(s)$ and $R_{33}(s)$ respectively.

As the 7-times current harmonic frequency was lower than f_d , substitute $k=7$ into the expression (10) to obtain:

$$\frac{j14\pi \cdot 700\pi K_{r7}}{(j700\pi)^2 + j14\pi \cdot 700\pi + (\omega_{r7})^2} = 0.994 + j0.109 \quad (12)$$

Solve Equation (12) and round the negative solution to get the frequency of characteristic angle $R_7(s)$. $\omega_{r7} = 701.544\pi$ rad/s and the resonance term coefficient $K_{r7} = 1.0061$.

As the 33-times current harmonic frequency was higher than f_d , substituted $k=33$ into the expression (11) to obtain:

$$\angle R_{33}(j3300\pi) = -\angle FC(j3300\pi) = 29.7^\circ \quad (13)$$

Solve Equation (13) to get the frequency of characteristic angle $\omega_{r33} = 3335.756\pi$ rad/s, thus obtaining $\angle Z_o(j\omega_{r33}) = -10.08^\circ$. Take a certain phase margin $PM = 20^\circ$ into account, substitute the values of $\angle Z_o(j\omega_{r33})$ and PM into Equation (8) to obtain:

$$K_{r33} = \sin(59.92^\circ) = 0.865 \quad (14)$$

Therefore, the characteristic angle frequency of $R_{33}(s)$ was $\omega_{r33} = 3335.756\pi$ rad/s, and the resonance term coefficient was $K_{r33} = 0.865$.

Similarly, it could design the quasi-resonance terms at the frequencies of fundamental wave and else current harmonics. All of the quasi-resonant parameters were shown in Table 1. The Bode plot of output impedance $Z_{o_tcwf}(s)$ was drawn to illustrate the situation when Time-Delay Compensation –

Weighted Feedforward Controlling Strategy in power grid voltage was applied on the grid connected inverter. It was shown in Figure 3, in comparison with $Z_{o_ff}(s)$, $Z_{o_tcwf}(s)$ possessed relatively higher amplitude at frequencies of the fundamental wave and current harmonics, which were lower than f_d band. Within the frequency band above f_d value, the phase was always above -90° . As a result, it proved that, the Time-Delay Compensation – Weighted Feedforward Controlling Strategy in power grid voltage could endow the grid-connected inverter with better inhibitory effect on current harmonics and greater adaptability in weak power grid.

Table 1 Design Results of the Quasi-Resonant Term

Harmonic frequency k	Coefficient of resonance term K_{rk}	Frequency of characteristic angle ω_{rk} (rad/s)
1	1.0001	100.031
3	1.001	300.283
5	1.003	500.786
7	1.006	701.544
13	0.583	1305.373
21	0.745	2114.331
33	0.865	3337.431

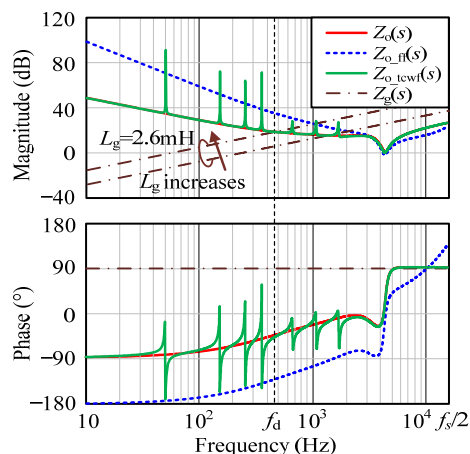


Figure 3 Bode Plot of the Grid Connected Inverter Output Impedance and the Power Grid Impedance

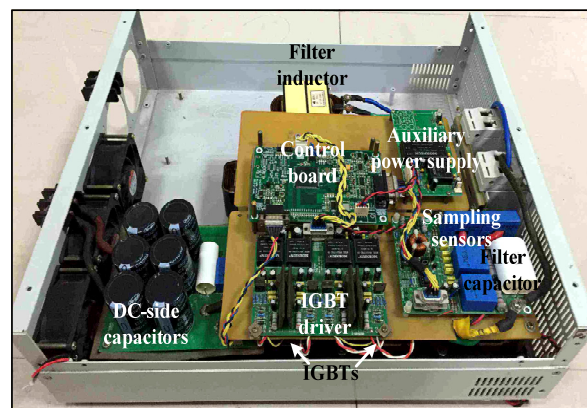


Figure 4 Prototype Picture of 6kW Mono-phase LCL Type Grid Connected Inverter

4. Experimental Validations

To prove the validity of power grid voltage Time-Delay Compensation - Weighted Feedforward Controlling Strategy mentioned in this thesis, a 6kW mono-phase LCL grid connected inverter prototype machine was built in the lab. It was shown in Figure 4. The main parameters were shown in Table 1. It selected IGBT module CM100DY-24NF as the switch transistor and selected M58962L chip as the switch transistor driver; In addition, Hall voltage sensor LV25-P was used to sampling the power grid voltage. Hall current sensor LA55-P was used to sampling the current through filter capacitor, and the grid-connected current. TMS320F2812 was selected as the digital processor; Through 14-bit AD IC MAX1324-ECM, the sampling signals were converted into digital signals then input into digital processor. In the meantime, the programmable AC power supply (Chroma 6560) was used to simulate the power grid voltage. Through serial connection of additional inductance, it simulated the impedance of power grid. The proposed method aimed at inhibiting the background

current harmonics in power grid from interfering with the grid-connected current. To validate its effect, it input 3-times, 5-times, 7-times, 13-times, 21-times and 33-times current harmonics into the power grid voltage respectively. The corresponding amplitude and phase to fundamental wave were shown in Table 3.

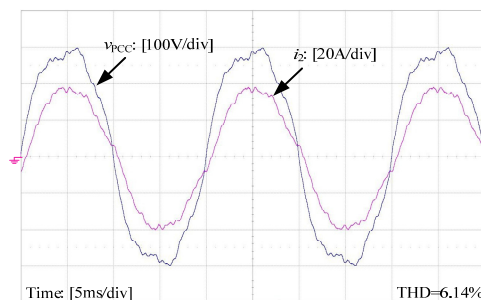
Table 2 Key Parameters of Grid Connected Inverter

Parameters	Value	Parameters	Value
Input Voltage V_{in}	380 V	Grid side inductance L_2	230 μH
Grid voltage V_g	220 Vrms	Triangular carrier amplitude V_{tri}	4.578V
Rated power S	6 kVA	Sampling rate f_s	30 kHz
Fundamental frequency f_o	50 Hz	Gi(s) proportional coefficient K_p	0.6725
Switching frequency f_{sw}	15 kHz	Gi(s) integral coefficient K_i	1400
Inverter side inductor L_1	720 μH	Sampling coefficient H_{i2}	0.15
Filter capacitance C	10 μF	Feedback coefficient H_{i1}	0.11

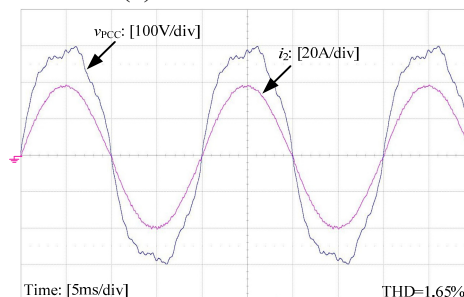
Table 3 Amplitude and Phase Corresponding to Fundamental Wave

Harmonic frequency	3	5	7	13	21	33
Amplitude	10%	5%	3%	1%	1%	1%
Phase	0°	-60°	0°	0°	0°	0°

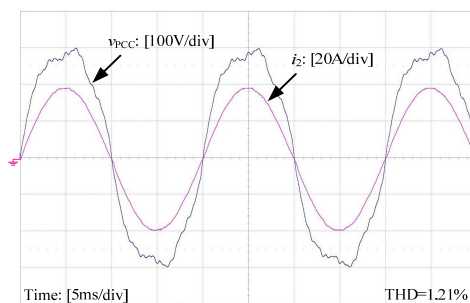
In Figure 5, the full-load experimental wave pattern regarding grid connected inverter was proposed. It used various strategies to control the inverter under high power grid. Figure 5(a) showed the experimental wave pattern when feedforward voltage was not applied in regulation. In this case, apparent current distortion was seen in grid-connected current as 6.14% THD. Figure 5(b) and 5(c) presented respectively the experimental wave patterns of full feedforward voltage control and Time-Delay Compensation – Weighted Feedforward Control in power grid voltage. In such cases, the wave pattern quality of grid-connected currents is excellent as 6.15% THD and 1.21% THD.



(a) No feedforward



(b) Full feedforward



(c) Time-Delay Compensation – Weighted Feedforward

Figure 5 Full-Load Experimental Wave Pattern by Various Feedforward Methods under High Power Grid

In Figure 6, it provided the content spectrums of respective current harmonics in three above mentioned controlling approaches. It showed that, when the power grid voltage Time-Delay Compensation – Weighted Forwardfeed strategy was applied, the grid-connected current harmonic content was the least. It is essential to point out that, within the grid-connected current, a part of low-frequency current harmonics were introduced by adding dead-time into the driving signal of the same leg switch transistor. Furthermore, this part of current harmonics couldn't be inhibited^[18] by feedforward voltage in power grid.

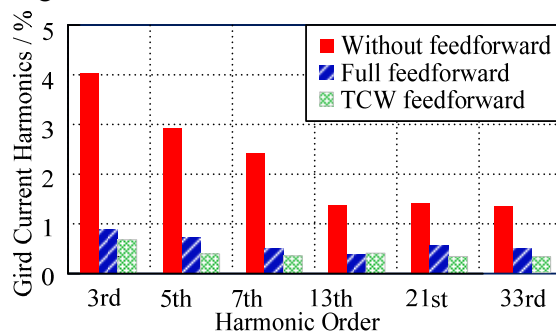


Figure 6 Current Harmonic Spectrums by Various Feedforward Strategies under High Power Grid

5. Conclusions

This thesis elaborated the influence that digital control delay acted on the grid connected inverter which was controlled by full feedforward grid voltage. Under such circumstances, the grid connected inverter couldn't take all effect to inhibit the current harmonics in connected grid. What is worse, it became unstable under the weak power grid. To solve above mentioned issues, this thesis proposed a Time-Delay Compensation and Weighted Feedforward Controlling Strategy in power grid voltage. It used the quasi-resonant term to extract the grid voltage at the frequencies of fundamental wave and the current harmonics, then proceeded feedforward. The quasi-resonant was designed to compensate the phase lag of cancellation term and to introduce appropriate feedforward weight. It juggled to ensure the system stability under weak power grid and guarantee the inhibitory effect on grid-connected current harmonics. Finally, a 6kW grid connected inverter was built in the lab to verify the validity of theoretical analysis and the proposed controlling strategy.

References

- [1] F. Baabjerg, R. Teodorescu, M. Liserre, and A. V. Timbus, "Overview of control and grid synchronization for distributed power generation systems," *IEEE Trans. Ind. Electron.*, vol. 53, no. 5, pp. 1398–1409, Oct. 2006.
- [2] M. Liserre, R. Teodorescu, and F. Blaabjerg, "Stability of photovoltaic and wind turbine grid-connected inverters for a large set of grid impedance values," *IEEE Trans. Power Electron.*, vol. 21, no. 1, pp. 263–272, Jan. 2006.

- [3] E. Twining and D. G. Holmes, "Grid current regulation of a three-phase voltage source inverter with an LCL input filter," *IEEE Trans. Power Electron.*, vol. 18, no. 3, pp. 888–895, May 2003.
- [4] M. Liserre, R. Teodorescu, and F. Blaabjerg, "Multiple harmonics control for three-phase grid converter systems with the use of PI-RES current controller in a rotating frame," *IEEE Trans. Power Electron.*, vol. 21, no. 3, pp. 836–841, May 2006.
- [5] M. Liserre, R. Teodorescu, and F. Blaabjerg, "Stability of photovoltaic and wind turbine grid-connected inverters for a large set of grid impedance values," *IEEE Trans. Power Electron.*, vol. 21, no. 1, pp. 263–272, Jan. 2006.
- [6] P. Xiao, K. A. Corzine, and G. K. Venayagamoorthy, "Multiple reference frame-based control of three-phase PWM boost rectifiers under unbalanced and distorted input conditions," *IEEE Trans. Power Electron.*, vol. 23, no. 4, pp. 2006–2017, Jul. 2008.
- [7] Y. A.-R. I. Mohamed, "Suppression of low- and high- frequency instabilities and grid-induced disturbances in distributed generation inverters," *IEEE Trans. Power Electron.*, vol. 26, no. 12, pp. 3790–3803, Dec. 2011.
- [8] X. Wang, X. Ruan, S. Liu, and C. K. Tse, "Full feedforward of grid voltage for grid-connected inverter with LCL filter to suppress current distortion due to grid voltage harmonics," *IEEE Trans. Power Electron.*, vol. 25, no. 12, pp. 3119–3127, Dec. 2010.
- [9] W. Li, X. Ruan, D. Pan, and X. Wang, "Full-feedforward schemes of grid voltages for a three-phase LCL-type grid-connected inverter," *IEEE Trans. Ind. Electron.*, vol. 60, no. 6, pp. 2237–2250, Jun. 2013.
- [10] D. Yang, X. Ruan, and H. Wu, "Impedance shaping of the grid-connected inverter with LCL filter to improve its adaptability to the weak grid condition," *IEEE Trans. Power Electron.*, vol. 29, no. 11, pp. 5795–5805, Nov. 2014.
- [11] D. Yang, X. Ruan, and H. Wu, "A real-time computation method with dual sampling modes to improve the current control performances of the LCL-type grid-connected inverter," *IEEE Trans. Ind. Electron.*, vol. 62, no. 7, pp. 4563–4572, July 2015.
- [12] X. Li, X. Wu, Y. Geng, X. Yuan, C. Xia, and X. Zhang, "Wide damping region for LCL-type grid-connected inverter with an improved capacitor-current-feedback method," *IEEE Trans. Power Electron.*, vol. 30, no. 9, pp. 5247–5259, Sep. 2015.
- [13] C. Chen, J. Xiong, Z. Wan, J. Lei, and K. Zhang, "A Time delay compensation method based on area equivalence for active damping of an LCL-type converter," *IEEE Trans. Power Electron.*, vol. 32, no. 1, pp. 762–772, Jan. 2017.
- [14] M. Lu, X. Wang, P. C. Loh, F. Blaabjerg, and T. Dragicevic, "Graphical evaluation of time-delay compensation techniques for digitally controlled converters," *IEEE Trans. Power Electron.*, vol. 33, no. 3, pp. 2061–2074, Mar. 2018.
- [15] K. Jalili and S. Bernet, "Design of LCL filters of active-front-end two-level voltage-source converters," *IEEE Trans. Ind. Electron.*, vol. 56, no. 5, pp. 1674–1689, May. 2009.
- [16] X. Ruan, X. Wang, D. Pan, D. Yang, W. Li, and C. Bao, *Control Techniques for LCL-Type Grid-Connected Inverters*. Berlin: Springer, 2017.
- [17] *IEEE Recommended Practice and Requirements for Harmonic Control in Electric Power Systems*, IEEE Standard 519-2014 (Revision of IEEE Standard 519-1992), Jun. 2014, p. 1–29.
- [18] X. Chen, X. Ruan, D. Yang, W. Zhao, and L. Jia, "Injected grid current quality improvement for voltage-controlled grid-connected Inverter," *IEEE Trans. Power Electron.*, vol. 33, no. 2, pp. 1247–1258, Feb. 2018.